

Specific heat of quantum Heisenberg model on a triangular lattice with two exchange parameters and its application to ^3He adsorbed on graphite

Y. R. Wang

Xerox Webster Research Center, 800 Phillips Road, 0114-41D, Webster, New York 14580

(Received 11 February 1992)

The quantum Heisenberg model on a triangular lattice with two exchange parameters, J between nearest-neighbor spins forming a Kagomé net, and ηJ between spins in the Kagomé net and ones at the center of each unit cell of the Kagomé net, is studied using the Wigner-Jordan transformation. The specific heat calculated from the model is found to have a double-peak structure when η is finite but substantially smaller than 1. The experimentally measured specific heat of the second-layer ^3He adsorbed on graphite can be explained in terms of our model calculation.

Recent specific-heat measurements of ^3He adsorbed on graphite at millikelvin temperatures by Greywall and Busch¹ have revealed some surprising results. Near densities corresponding to the completion of second-layer adsorption, the specific heat shows a peak at 2.5 mK, whereas the entropy calculated from the specific-heat data, integrated from zero temperature through this peak assuming a linear temperature dependence of the specific heat below 2 mK, is only approximately $\frac{1}{2} k_B \ln 2$, one-half of the expected value. The peak position is rather insensitive to the areal density. The missing entropy, together with magnetization measurements,² seems to strongly suggest the existence of a second peak (or a shoulder) in the specific heat below 2 mK. This interesting behavior of the heat capacity is apparently associated with the second-layer ^3He nuclear-spin-exchange interactions since the first-layer ^3He atoms are highly compressed and therefore contribute very little to the specific heat.¹ The exchange interactions among the second-layer ^3He nuclear spins are likely to be antiferromagnetic (AFM), as suggested from the magnetization measurements.²

Since the first-layer ^3He atoms form a triangular lattice, at appropriate densities a solid phase of the second-layer ^3He atoms registered with respect to the first layer may also form.³ Elser⁴ noticed that at the density $\rho = 0.178/\text{\AA}^2$ the ratio of the second-layer density ($0.064/\text{\AA}^2$) to the first layer density, 0.56, is close to the fraction $\frac{4}{7}$, and therefore suggested a $\sqrt{7} \times \sqrt{7}$ triangular structure that has two types of atoms, one residing on the saddle points between adjacent dimples in the first layer, with the other directly above a first-layer atom. A quantum Heisenberg model on a Kagomé net is suggested⁴ to explain the heat-capacity puzzles. Roger,⁵ on the other hand, emphasizes the importance of the higher-order ring exchange processes, whereas Machida and Fujita⁶ invoke the lattice-gas model. Various models are all studied⁴⁻⁶ using numerical methods with small systems, and double peak structures of the specific heat are found. The position of the lower temperature peak in these calculations, however, is about an order of magnitude lower than that of the higher one. Since the boundary effects will be very significant at such low temperatures, the double peak structure of the specific heat may not be intrinsic to the

models, but an artifact of the finite-size calculations, a possibility also noticed by the authors^{4,5} In this paper we study the quantum Heisenberg model on a triangular lattice with two different exchange parameters, J between spins forming a Kagomé net and ηJ between spins in the Kagomé net and ones at the center of the unit cell of the Kagomé net, using the two-dimensional (2D) Wigner-Jordan (WJ) transformation developed recently.^{7,8} The double peak structure of the specific heat is found for a disordered (spin liquid) state, and is interpreted as the result of a small but finite η . A simple interpretation of the missing entropy emerges as to be associated with the "exhaustion" of the states below 2 mK from the exchange interaction ηJ . The position of the "high" temperature peak is shown to be insensitive to the ratio of the two exchange parameters, implying the insensitivity to the areal density observed experimentally. The heat-capacity puzzle of the second-layer ^3He near density of $0.178/\text{\AA}^2$ can therefore be explained rather coherently. While our results support the notion suggested by Elser⁴ that the heat-capacity puzzle may be understood from the quantum Heisenberg model on a triangular lattice, without invoking higher-order ring-exchange processes, they differ from Elser's results in several significant ways. First, Zeng and Elser^{4,9} attribute the double peak structure of the specific heat to the quantum AFM Heisenberg model on a Kagomé net ($\eta = 0$), whereas in our study we find that the heat capacity of the quantum spins on a Kagomé net is only singly peaked, and that at low temperatures the specific heat of the spins on a Kagomé net is linearly proportional to temperature. Second, while the position and the shape of the high-temperature peak is in excellent agreement with calculations by Zeng and Elser,^{4,9} our interpretation of the nature of the peak is different. In terms of our interpretation, the peak is not an unusual one. It signals that at the peak temperature all spin degrees of freedom are thermally accessible. Therefore at temperatures much higher than the peak temperature the specific heat decreases as $1/T^2$ (recall that specific heat is a derivative of the internal energy with respect to temperature), and below the peak temperature the specific heat also decreases since less states become thermally accessible. The interpretation of the low-temperature peak is

similar. At that peak all the states related with interactions (ηJ) between the inequivalent spins are thermally accessible. Thus in terms of our interpretation, the peaks do not signal condensations to different states, in contrast to that speculated by Elser.⁴ In fact, the spins remain in a disordered state at all finite temperatures.

The study of the quantum Heisenberg model on a triangular lattice with two exchange parameters is interesting in its own right. Spin-wave calculations^{9,10} have shown that the number of spin waves from zero point vibrations is large because of geometrical frustration, and for η less than 0.2, spin-wave calculations show that the sublattice magnetization is smaller than zero, a pathological result.⁹ A large number of spin waves from zero point vibrations indicates that the quantum spin identities, $S_i^+ S_i^- + S_i^- S_i^+ \equiv 1$, are not satisfied.¹¹ It is therefore important to develop other methods to study the model. Methods developed based on the 2D Wigner-Jordan transformation have shown to be promising alternatives.⁷ In particular, when applied to the isotropic antiferromagnetic Heisenberg model on a triangular lattice,¹² the method yields a spin liquid state which has a ground-state energy lower than that calculated from spin-wave theories, yet almost identical to that calculated from direct diagonalization of small systems. Here we generalize the method to include the quantum Heisenberg model on a triangular lattice with two exchange parameters.

The generalization, however, is a rather nontrivial task, and therefore will be discussed briefly below. The unit cell of the $\sqrt{7} \times \sqrt{7}$ lattice is shown in Fig. 1. Atoms A , B , and C are sitting on the saddle points between adjacent dimples of the first-layer atoms, and atom D is sitting directly on top of a first-layer atom. Atoms A , B , and C form a Kagomé net, and D is at the center of each unit cell. The thick lines designate nuclear-spin-exchange interaction, J , between A , B , and C atoms, whereas the thin lines represent the exchange interaction, ηJ , between D and A , B , and C (we shall call it the interaction between inequivalent spins). We expect J to be positive (i.e., antiferromagnetic), and the magnitude of η less than 1. The Heisenberg model is then

$$H = J \sum_{ij} \mathbf{S}_i \cdot \mathbf{S}_j + \eta J \sum_{in} \mathbf{S}_i \cdot \mathbf{S}_n, \quad (1)$$

where the first summation is over the Kagomé net, and the

$$H_{\text{MF}} = 2J(1+2\Delta_1) \sum_{\mathbf{k}} (A_{\mathbf{k}}^\dagger B_{\mathbf{k}} \text{sinc} \cdot \boldsymbol{\tau}_1 + A_{\mathbf{k}}^\dagger C_{\mathbf{k}} \text{sinc} \cdot \boldsymbol{\tau}_2 + B_{\mathbf{k}}^\dagger C_{\mathbf{k}} \text{sinc} \cdot \boldsymbol{\tau}_3 + \text{H.c.}) \\ + 2\eta J(1+2\Delta_2) \sum_{\mathbf{k}} (A_{\mathbf{k}}^\dagger D_{\mathbf{k}} \text{sinc} \cdot \boldsymbol{\tau}_3 + B_{\mathbf{k}}^\dagger D_{\mathbf{k}} \text{sinc} \cdot \boldsymbol{\tau}_2 + C_{\mathbf{k}}^\dagger D_{\mathbf{k}} \text{sinc} \cdot \boldsymbol{\tau}_1 + \text{H.c.}) + 3NJ\Delta_1^2 + 3N\eta J\Delta_2^2, \quad (2)$$

where $A_{\mathbf{k}}$, $B_{\mathbf{k}}$, $C_{\mathbf{k}}$, and $D_{\mathbf{k}}$ are the WJ fermion annihilation operators at the respective sublattices, as shown in Fig. 1, and $\boldsymbol{\tau}_1$, $\boldsymbol{\tau}_2$, and $\boldsymbol{\tau}_3$ are the nearest-neighbor vectors of the triangular lattice. The mean-field Hamiltonian can be diagonalized using various methods. The complication, however, comes from the self-consistent conditions:

$$\Delta_1 = \frac{1}{N/4} \sum_{\mathbf{k}} \langle B_{\mathbf{k}} A_{\mathbf{k}}^\dagger \rangle \text{sinc} \cdot \boldsymbol{\tau}_1 = \frac{1}{N/4} \sum_{\mathbf{k}} \langle C_{\mathbf{k}} A_{\mathbf{k}}^\dagger \rangle \text{sinc} \cdot \boldsymbol{\tau}_2, \quad (3a)$$

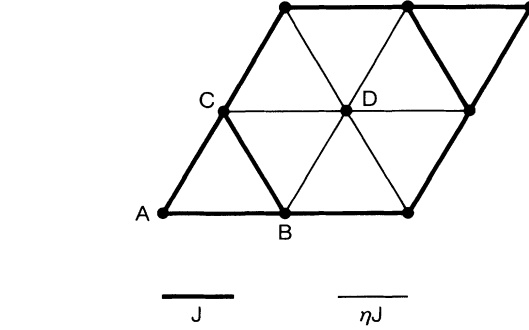


FIG. 1. Unit cell of the $\sqrt{7} \times \sqrt{7}$ registered phase of the second-layer ^3He adsorbed on graphite. Atoms A , B , and C form a Kagomé net. The thick lines designate the exchange interaction J , and the thin lines ηJ .

second over the nearest-neighbor spins connected by the thin lines. We first transform the spin variables into spinless fermion variables, i.e., $S_i^- = d_i \exp[i(\phi_i - \phi_i^0)]$, where d_i is a fermion annihilation operator at site i , and $\phi_i = \sum_{j \neq i} d_j^\dagger d_j B_{ij}$ [$B_{ij} \equiv \text{Im} \ln(\tau_j - \tau_i)$, where $\tau_j = x_j + iy_j$ is the complex coordinate of the j th spin]. The local gauge phase, ϕ_i^0 , can be any real function of the site index i . This local gauge invariance can be used to minimize fluctuations around a particularly chosen mean-field solution, and for the triangular lattice, the choice of $\phi_i^0 = \frac{1}{2} \sum_{j \neq i} B_{ij}$ has been shown to be a good one.¹² The z component of the spin operator is related to the number operator of the WJ fermions, $S_i^z = d_i^\dagger d_i - \frac{1}{2}$. In a spin state where the z component of the spins is zero on average, which is indeed the case for the triangular lattice, $\langle d_i^\dagger d_i \rangle = \frac{1}{2}$. We next proceed to find a mean-field solution of the transformed Hamiltonian by defining two nearest-neighbor bonding fields: $\Delta_{1,ij} \equiv \langle d_i d_j^\dagger \rangle = \Delta_1 e^{i\theta_{ij}}$ for i and j belonging to the Kagomé net, and $\Delta_{2,in} \equiv \langle d_i d_n^\dagger \rangle = \Delta_2 e^{i\theta_{in}}$ for n belonging to the center of a unit cell of the Kagomé net. The phase θ_{ij} (and θ_{in}) is either $\pi/2$ or $-\pi/2$, depending¹² on the relative positions of sites i and j , as can be self-consistently determined below. Δ_1 and Δ_2 can be approximately considered as the bonding amplitude between nearest-neighbor spins.¹² The reduced mean-field Hamiltonian can be written as

$$\Delta_2 = \frac{1}{N/4} \sum_{\mathbf{k}} \langle D_{\mathbf{k}} A_{\mathbf{k}}^\dagger \rangle \text{sinc} \cdot \boldsymbol{\tau}_3 = \frac{1}{N/4} \sum_{\mathbf{k}} \langle D_{\mathbf{k}} B_{\mathbf{k}}^\dagger \rangle \text{sinc} \cdot \boldsymbol{\tau}_2, \quad (3b)$$

$$\frac{1}{N/4} \sum_{\mathbf{k}} \langle B_{\mathbf{k}} A_{\mathbf{k}}^\dagger \rangle \text{cosk} \cdot \boldsymbol{\tau}_1 = \frac{1}{N/4} \sum_{\mathbf{k}} \langle D_{\mathbf{k}} C_{\mathbf{k}}^\dagger \rangle \text{cosk} \cdot \boldsymbol{\tau}_1 = 0, \quad (3c)$$

and

$$\frac{1}{N/4} \sum_{\mathbf{k}} \langle A_{\mathbf{k}}^\dagger A_{\mathbf{k}} \rangle = \frac{1}{N/4} \sum_{\mathbf{k}} \langle D_{\mathbf{k}}^\dagger D_{\mathbf{k}} \rangle = \frac{1}{2}. \quad (3d)$$

We find that it is most convenient to diagonalize the Hamiltonian and obtain the thermally averaged occupation number and the bonding amplitudes by using the Green's-function method. Equation (3d) requires that the states are half filled by the WJ fermions. Δ_1 and Δ_2 are calculated for the half-filled band from Eqs. (3a) and (3b), and the self-consistency conditions (3c) and (3d) are shown satisfied by numerical evaluations. The mean-field energy is

$$E \equiv E_1 + E_2 = -3NJ\Delta_1(1 + \Delta_1) - 3N\eta J\Delta_2(1 + \Delta_2). \quad (4)$$

E_1 can be considered as a contribution from bonding between spins in the Kagomé net, and E_2 that from bonding between inequivalent spins. The specific heat is finally calculated from E by taking derivatives with respect to the temperature.

The spin state described by the above mean-field solution is a disordered (i.e., liquid) state in the sense that no preferred spin directions are given in the solution. The excitation spectrum is gapless for all the η values, which in the $\eta=0$ case (the Kagomé net) agrees with numerical calculations.^{4,9} The absence of long-range order in a $S = \frac{3}{2}$ AFM Kagomé lattice has been experimentally observed¹³ down to a very low temperature, giving further support of the spin liquid state for the present case ($S = \frac{1}{2}$).

The specific heat and the entropy calculated from the above self-consistent mean-field solution is shown in Fig. 2 for $\eta=0.4$. The dashed curve in the figure is $C_2(T) = dE_2/dT$, i.e., the contribution to the specific heat from bonding between inequivalent spins. A double peak structure is clearly seen in the specific-heat curve, one at $T/2J \approx 0.67$ and the other at $T/2J \approx 0.05$, for $\eta=0.4$. While the position of the low-temperature peak changes with η significantly, that of the high-temperature peak

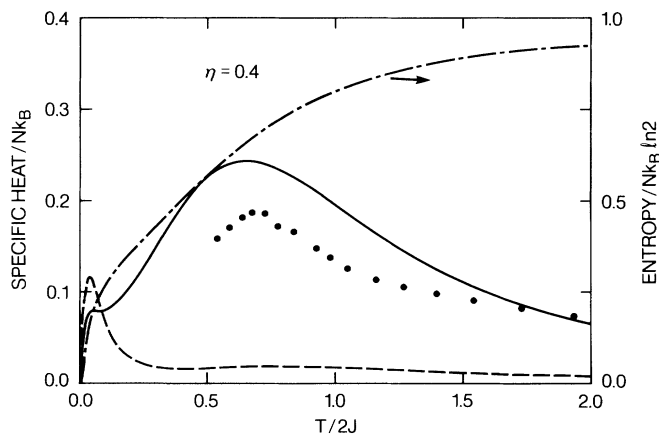


FIG. 2. Specific heat (solid and dashed curves) and entropy (dash-dotted curve) calculated for the case $\eta=0.4$. The dashed curve is the specific heat contributed from bonding between the spins in the Kagomé net (A , B , and C in Fig. 1) and those at the center of each unit cell of the Kagomé net (D in Fig. 1). The solid circles are the experimental specific heat of second-layer nuclear spins of ^3He adsorbed on graphite in the unit of Nk_B , where N is computed from the second-layer areal density $0.064/\text{\AA}^2$, and the surface area of 203 m^2 (Ref. 1).

does not. Figure 3 shows the specific heat of two extreme cases, $\eta=1$ (isotropic Heisenberg) and $\eta=0$ (Kagomé net). In both cases the specific heat is only singly peaked. The peak position of the Kagomé net is at $T/2J \approx 0.65$, in excellent agreement with numerical calculations,^{4,9} and that of the isotropic Heisenberg model is at $T/2J \approx 0.75$. The shape of the high-temperature peak is sharpened when η decreases, and for $\eta=0$, the specific heat below the peak is linear in temperature. The peaks are not related to phase transitions. We have calculated the temperature dependence of the mean fields, Δ_1 and Δ_2 , and found that they are smooth functions at any finite temperature.

The experimental specific heat of the second-layer ^3He near density $0.178/\text{\AA}^2$ is peaked at 2.5 mK and can be presented as linear in temperature from 2 to 2.5 mK. This suggests that the exchange interaction between inequivalent spins is significantly smaller than that between the spins in the Kagomé net (we expect $\eta < 0.5$ to be likely). The insensitivity of the experimental peak position with respect to coverage may be explained in terms of the insensitivity of the high-temperature peak position with respect to η in our calculation. For densities near $0.178/\text{\AA}^2$, the registered phase will contain vacancies or interstitials. It is likely that the vacancies or interstitials will go to the center sites (the D atoms in Fig. 1) since the D atoms are directly located on top of first-layer atoms, leaving the atoms in the Kagomé net not significantly changed. Since the position of the high-temperature peak from our calculation is mainly related to the spin interactions between the atoms in the Kagomé net, little change in the position of the specific heat is expected. Quantitative comparison between theory and experiment is shown in Fig. 2. The experimental data¹ are shown for the case of $\rho = 0.178/\text{\AA}^2$, a surface area of 203 m^2 , and assuming all the atoms contribute to the nuclear-spin specific heat. A value of $2J \approx 3.7 \text{ mK}$ is obtained from the comparison. While the shape of the experimental peak is comparable with our calculated one, the theoretical value at the peak is about 30% larger than the experimental one. At high temperatures the experimental data do not decrease as $1/T^2$, in contrast to that suggested by the present as well

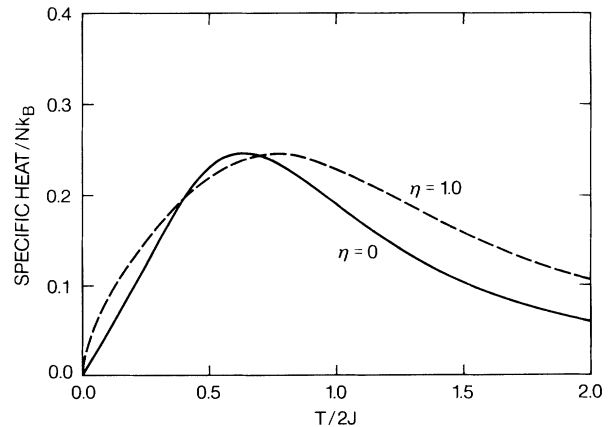


FIG. 3. Specific heat calculated for the quantum Heisenberg model on a Kagomé net ($\eta=0$, solid curve) and on an isotropic triangular lattice ($\eta=1$, dashed curve).

as previous^{4,5} theories. The two problems might be related to the amount of vacancies and interstitials present in the experiment which locally melt the solid phase, and thus only contribute to the specific heat at high temperature. Experimental evidence for a liquid component has been noted previously.¹

A more striking result from our theoretical calculation is the interpretation of the missing entropy. The high-temperature entropy of the spins in a pure Kagomé net ($\eta=0$), obtained by integrating the specific heat (solid curve in Fig. 3) from 0 to a temperature much larger than $2J$, is $\frac{3}{4} k_B \ln 2$ per atom. This is expected since there are four atoms in each unit cell, but only three atoms belong to the Kagomé net. When we turn on the exchange interaction between the inequivalent spins, i.e., when $\eta \neq 0$, no matter how small η is, the high-temperature entropy contributed from the bonding between the spins in the Kagomé net, $S_1 = \int_0^\infty [C_1(T)/T] dT$, where $C_1(T) = dE_1(T)/dT$, is only $\frac{1}{2} k_B \ln 2$ per atom. The missing other one-half of the entropy comes from the bonding between inequivalent spins: $S_2 = \int_0^\infty [C_2(T)/T] dT = \frac{1}{2} k_B \ln 2$ per atom, independent of η . Thus for any finite η , the spin degrees of freedom are equally distributed among the

“bonds” formed between nearest-neighbor spins. There are six “heavy” bonds (J) per unit cell from the spins in the Kagomé net, and six “light” bonds (ηJ) formed between inequivalent spins, each contributing one-half of the total entropy. For $2J \approx 3.7$ mK, and $\eta < 0.5$, the spin degrees of freedom associated with the light bonds are exhausted below 2 mK. The temperature dependence of the entropy is calculated for $\eta=0.4$ in Fig. 2.

In summary, we have shown that the specific heat of the quantum Heisenberg model on a triangular lattice with two exchange parameters exhibits a double peak structure when one exchange parameter is finite but substantially smaller than the other. The high-temperature peak is mainly a property of the exchange interactions between the spins in the Kagomé net, and is thus to a large degree insensitive to the other exchange interactions. The entropy at high temperature is equally contributed from both exchange interactions. These findings qualitatively explain the experimental specific-heat puzzle of the second-layer ³He adsorbed on graphite.

The author is grateful to Dr. D. S. Greywall for helpful discussions of the experimental data.

¹D. S. Greywall and P. A. Busch, Phys. Rev. Lett. **62**, 1868 (1989); D. S. Greywall, Phys. Rev. B **41**, 1842 (1990).

²H. Franco, R. E. Rapp, and H. Godfrin, Phys. Rev. Lett. **57**, 1161 (1986).

³S. W. Van Sciver and O. E. Vilches, Phys. Rev. B **18**, 285 (1978).

⁴Veit Elser, Phys. Rev. Lett. **62**, 2405 (1989).

⁵M. Roger, Phys. Rev. Lett. **64**, 297 (1990).

⁶K. Machida and M. Fujita, Phys. Rev. B **42**, 2673 (1990).

⁷Y. R. Wang, Phys. Rev. B **43**, 3786 (1991); **43**, 13774 (1991); Y. R. Wang, M. J. Rice, and H. Y. Choi, *ibid.* **44**, 9743

(1991).

⁸J. Ambjorn and G. Semenoff, Phys. Lett. B **226**, 107 (1989); E. Fradkin, Phys. Rev. Lett. **63**, 332 (1989); E. J. Mele, Phys. Scr. **T27**, 82 (1989).

⁹C. Zeng and V. Elser, Phys. Rev. B **42**, 8436 (1990).

¹⁰Th. Jolicoeur and J. C. Le Guillou, Phys. Rev. B **40**, 2727 (1989).

¹¹Y. R. Wang and M. J. Rice, Phys. Rev. B **45**, 5045 (1992).

¹²Y. R. Wang, preceding paper, Phys. Rev. B **45**, 12604 (1992).

¹³C. Broholm, G. Aeppli, G. P. Espinosa, and A. S. Cooper, Phys. Rev. Lett. **65**, 3173 (1990).